The role of diversity in mediating microbiota structural and functional responses in two sympatric species of abalone under stressed withering syndrome conditions

Francesco Cicala
CICESE: Centro de Investigacion Cientifica y de Educacion Superior de Ensenada
José Alejandro Cisterna-Céliz
CICESE: Centro de Investigacion Cientifica y de Educacion Superior de Ensenada
Marcos Paolinelli
Consejo Nacional de Investigaciones Cientificas y Tecnicas
James D. Moore
University of California Davis Bodega Marine Laboratory
Joseph Sevigni
University of New Hampshire
Axayacatl Rocha-Olivares (arocha@cicese.mx)
Centro de Investigacion Cientifica y de Educacion Superior de Ensenada https://orcid.org/0000-0002-2700-9086

Research

Keywords: Microbiota, structural composition, functional perdition, Withering Syndrome, Insurance hypothesis, Anna Karenina principle, Haliotis corrugata, Haliotis fulgens, 454 pyrosequencing, PICRUSt

Posted Date: March 15th, 2021

DOI: https://doi.org/10.21203/rs.3.rs-281891/v1

Abstract

Background: The withering syndrome (WS) is an infectious disease initially affecting the gastro-intestinal tract (GI) of wild abalone populations of the coasts of Baja California. In spite of its high incidence, structural and functional changes in abalone GI microbiotas under WS-stressed conditions remain poorly investigated. Moreover, it is equally uncertain if interspecific microbiota features, such as the presence or absence of certain bacterial species, their abundances, and their functional capabilities, may prevent or at least lead to different microbiota responses. Healthy *Haliotis fulgens* and *Haliotis corrugata* from Baja California Sur (Mexico) harbor species-specific structural and functional microbiota profiles; hence, we hypothesize a distinctive microbiota response under WS-stressed conditions. Here, we compared both the structural arrangements and functional capabilities of healthy and dysbiotic microbiotas using 454 pyrosequencing high throughput sequencing technologies and PICRUSt v.2 outputs, respectively.

Results: Our findings suggest that the extent to which WS may involve structural and functional changes in GI microbiotas is contingent on the microbiota diversity itself. Indeed, we report significant structual alterations in the less complex microbiotas of *H. fulgens*, which in turn led to a significant downregulation of several metabolic activities conducted by GI bacteria. Conversely, the effects of WS were marginal in more complex bacterial communities, as in *H. corrugata*, in which no significant structural and functional changes were detected.

Conclusions: Our results provide new insights concerning the role of microbiome diversity in abalone health and the etiology of WS. Notably, complex bacterial communities appear to be less affected by WS than less complex microbiotas. Moreover, our insights suggest that structural changes observed under WS-stressed conditions may be considered stochastic, as predicted by the Anna Karenina principle, and result in the downregulation of several ecological functions conducted by GI bacteria. Overall, our results support the hypothesis that the occurrence of WS may be associated with shifts in GI microbiotas. Moreover, we propose that the susceptibility to WS that has been reported among abalone species may reflect the natural degree of complexity of the GI microbiomes harbored by each species.

Background

Wild abalone (*Haliotis* spp.) populations are in decline worldwide due to overexploitation and natural causes, such as epidemic disease outbreaks [1]. Reductions in the populations of these species may result in both strong economic losses and unpredictable ecological impacts. Adult abalone are considered ecosystem engineers, as they graze macro- and microalgae and thus maintain open habitats that may be exploited by other organisms [2–4]. Moreover, these gastropods support valuable fisheries in many countries worldwide [5–7]. The peninsula of Baja California harbors seven exploitable abalone species [8], although the harvest is focused almost entirely on the blue abalone *Haliotis fulgens* (HF) and the yellow abalone *Haliotis corrugata* (HC) [8,9]. In recent decades, the main disease contributing to the decline of wild Mexican abalone populations has been withering syndrome (WS), a chronic and fatal disease that has been responsible for moderate and massive mortality events [10,11]. Notably, the degree

of susceptibility and occurrence of this disease varies among abalone species and the causes of WS remain poorly understood [1,3,7].

Early studies of WS have linked the occurrence of this syndrome with infection by a GI intracellular *Anaplasmataceae* bacterium [12] of the order *Rickettsiales* named *Candidatus* Xenohaliotis californiensis (*C*Xc) [13]. The primary findings supporting the connection between WS and *C*Xc have resulted from the identification of this novel bacterium using microscopic (in situ hybridization) and molecular (*16S rRNA* gene) techniques with histological inclusions of infected abalone [13]. Moreover, diseased abalone with clinical signs of WS have been found to regain their original health status after treatment with a *Rickettsiales*-killing antibiotic [13]. Nevertheless, recent studies have weakened such correlations, and *C*Xs-WS co-occurrence remains a topic of debate. Specifically, histological analyses have revealed the presence of *C*Xc inclusions in both diseased and healthy abalone with similar prevalence ranges [14,15]. Moreover, the absence of *C*Xc in WS-stressed abalone has also been recorded, suggesting that WS may be trigged by additional pathogenic microbes [16–18].

Novel insights regarding animal microbiotas have revealed that microorganism symbiosis is ubiquitous in metazoans, and the understanding of such partnerships is redefining our knowledge of animal biology [19]. Bacterial microbiotas carry out essential physiological activities that influence the health, development, disease susceptibility, and the behavior of their hosts [20–22]. In this regard, the study of gastro-intestinal (GI) microbiotas has become a growing area of research, and it has become increasingly accepted that GI microbiotas and their associated gene pools play pivotal roles in the overall health of host species [23]. Thus, understanding changes in GI microbiomes and the consequences for their hosts represents one of the main goals in microbial ecology [20].

In this context, the Insurance hypothesis proposed by Yachi and Loreau [24], suggests that the community-level variance would decrease as diversity increases due to both, the possibility that different species may respond differentially to environmental changes and with increased redundancy levels (i.e., different species may carry out the same ecological function) [24–26]. The latter appears to be particularly relevant in GI microbiotas, as high diversity has direct consequences on the health status of the host [27]. Moreover, shifts in associated bacterial communities have been linked to epidemiologic outbreaks in different marine invertebrates [28,29]. Furthermore, recent observations suggest that, under normal circumstances, microbiome arrangements tend to favor a small number of beneficial configurations. Accordingly, stressors and disease will lead to stochastic rather than deterministic changes in the microbiome, which consequently result in a higher number of unpredictable microbiota configurations. These observations have led to the Anna Karenina principle (AKP), whose name comes from the opening sentence of Anna Karenina by Leon Tolstoy: "*All happy families are all alike; each unhappy family is unhappy in its own way.*" In 2017, Zaneveld et al. [20] rephrased this sentence and created an ecological host-associated microbiome hypothesis: "*All healthy microbiomes are similar; each dysbiotic microbiome is dysbiotic in its own way.*"

Although these theories appear common and important for the overall health of the host, little information is available for invertebrate microbiomes, particularly those from marine environments [30–32]. In abalone species, only an exiguous number of studies have thus far evaluated structural alterations in the microbiotas of abalone with WS [32]. Consequently, the extent to which WS may be involved in structural and functional alterations in abalone GI bacterial communities remains unclear. In addition, the hypothesis that species-specific microbiota arrangements among abalone species may lead to different abalone responses to WS remains unexplored. Recently, we compared and reported the structural arrangements and functional capability profiles for the GI microbiotas of healthy HC and HF [33]. The microbiotas of HF appears to be less complex compared to that of HC, as it is mainly dominated by *Mycoplasma* spp., whereas the microbiotas of HC appears to be composed by a higher number of bacterial operational taxonomic units (OTU) species [33]. Here, we posited that these microbiota characteristics may lead to microbiota-specific responses in WS-stressed abalone and that dysbiotic microbiotas would be characterized by a high number of new stochastic bacterial configurations, as predicted by the aforementioned ecological theories.

Methods

Sample collection, DNA extraction, and PCR amplification

Commercially harvested wild abalone were collected in April and November of 2012 during two field expeditions conducted along the Pacific coast of Baja California Sur (Mexico; Additional file 1: Table S1). In the field, landed abalones were morphologically inspected to identify animals bearing morphological signs of WS including low mobility, color alterations, and pedal muscle and mantle retraction, as proposed by Friedman [34]. After the morphological examination, approximately 30 mg of post-esophageal tissue was collected from each of the 107 abalone included in the study (n = 46 for HC; n = 61 for HF). Specimens were immediately transferred to sterile 1.5-ml microcentrifuge tubes containing molecular grade ethanol until further analysis.

In the laboratory, DNA was extracted and purified from preserved tissues using a DNeasy blood & tissue kit (Qiagen, Valencia, CA, USA) following the protocol of the manufacturer. PCR amplification of an internal fragment of the *16S rRNA* gene spanning the V1-V3 regions (~500 bp) was conducted using universal eubacterial primers 28F (5’ – GAGTTTGATCNTGGCTCAG – 3’) [35] and 519R (5’ – GTNTTACNGCGGCKGCTG – 3’) [36]. Amplifications were carried out in 20-μl reactions containing 100 ng of DNA, 1X PCR buffer, 1.5 mM $MgCl_2$ (Kapa Biosystems, Woburn, MA, USA), 0.2 mM dNTPs (New England Biolabs, Beverly, MA, USA), 0.3 μM of each primer, and 1U of Taq polymerase (Kapa Biosystems, Woburn, MA, USA). The thermal cycling conditions were 94 °C for 4 min, followed by 40 cycles of 94 °C for 1 min, 62 °C for 30 s, 72 °C for 30 s, and a final extension of 8 min at 72 °C. Confirmation of amplification was carried out by 1.5% agarose gel electrophoresis.

16S rRNA gene library preparation

PCR amplicons were sent to the Research and Testing Laboratory (Lubbock, TX) for pre-sequencing preparation and Roche 454 pyrosequencing. Briefly, the amplicons were tagged using Roche 454 adaptors and multiplex identifier (MID) tags for each organism, following the bacterial tag-encoded FLX amplicon pyrosequencing (bTEFAP) approach of Dowd *et al.* [37]. Roche 454 pyrosequencing was carried out in a GS FLX Titanium platform. The raw *16S rRNA* gene libraries were processed as follows: 1) the SFF files were formatted into FASTA sequences and quality files; 2) the reads were demultiplexed from SFF files using the Roche sffinfo tool; 3) low quality bases (Phred score < 25), primers, and barcode sequences were removed using a Research and Testing Laboratory internal quality trimming algorithm; and 4) dereplication was carried out using the USEARCH algorithm [38]. The raw reads were deposited in the National Center for Biotechnology Information (NCBI; BioProject: PRJNA494699, accession number: SRR7969002).

The returned reads were processed and analyzed using Quantitative Insights Into Microbial Ecology v. 2019.4 – 2019.7 (QIIME2) [39]. After importing into QIIME2, the reads were *de novo* clustered into OTUs at 97% identity using the QIIME vsearch cluster-features-de-novo plugin [40]. Chimeras and singletons were detected and removed using UCHIME [41] and the filter-features plug in implement in QIIME2 v.2019-7, respectively. We organized two control steps in order to minimize PCR amplicon noise. Initially, the taxonomic assignments of the OTUs were conducted via a classify-consensus-blast [42] trained on *16S rRNA* gene OTUs clustered at 99% similarities within the Silva_132 database [43], and unreliable sequences with no match in the SILVA_132 database (e.g., unassigned) were removed before further analyses. Additionally, we removed reads with frequencies inferior to 0.005% [44]. As a result, OTUs with total read numbers < 4 were removed from both the HF and HC data sets.

Finally, the reads were rarefied by randomly subsampling at 702 and 644 reads for HF and HC, respectively. We selected those sampling depths in order to minimize the loss of both specimens and bacterial diversity. The selected rarefaction values were as close as possible to the asymptotic plateau of the rarefaction curves for both species (Additional file 2: Fig. S1a and Fig. S1b), which also allowed for the retention of most abalone. The number of removed reads and OTUs during each quality control step, as well as the final numbers of reads and OTUs used as input in downstream analyses are reported in Additional file 1: Table S2.

Ecological analyses

To evaluate how exhaustively the bacterial communities were sampled, rarefaction curves of the detected OTUs were generated using the diversity alpha-rarefaction plugin implemented in QIIME2 v. 2019.7 [39] for each abalone. Also, the number of OTUs obtained was compared against the non-parametric species richness estimator Chao 1 (Additional file 2: Fig. S1c) [45].

Microbiome community structure was evaluated by principal coordinate analysis (PCoA) based on Bray Curtis, Jaccard, and weighted and unweighted phylogenetic Unifrac distance metrics obtained from the abundance of each rarefied OTU. The PCoA results were visualized with EMPeror [46]. Statistical

differences were evaluated by a permutational multivariate analysis of variance (PERMANOVA) based on 4999 permutations using the beta-group-significance plugin of QIIME2 v.2019.7 [47]. Additionally, the multivariate dispersion based on OTU abundance in morphological categories was estimated by a permutation analysis of multivariate dispersion (PERMDISP) with 4999 permutations implemented in PRIMER+P v.6 [48].

At the OTU taxonomic level and with the aim to include all shared bacterial OTUs and/or exclusive non-rarefied OTUs between morphologically healthy and WS-stressed abalone, the OTUs were visualized using Venn diagrams created with open web-software InteractiVenn [49]. Also, the differential abundance of rarefied OTUs between healthy and WS afflicted abalone was determined by linear discriminant analysis (LDA) effect size (LEfSe) [50]. Finally, to determine which OTUs primarily contributed to the dissimilarity between both proposed categories, a similarity percentage (SIMPER) analysis based on rarefied OTU abundance was conducted using PRIMER+P v.6 [48].

Functional prediction

We used PICRUSt v.2.2.0 beta [51] to predict both the potential functional capabilities and the contributions of distinct OTUs to Kyoto Encyclopedia of Genes and Genomes (KEGG) pathways. Briefly, the OTUs were normalized by the predicted *16S rRNA* gene copy number of each OTU. To implement quality control, we computed the nearest sequenced taxon index (NSTI). Briefly, the NSTI evaluates the prediction accuracy of PICRUSt since it reflects the average genetic distance (measured as the number of substitutions per site) between each OTU against that of the *16S rRNA* gene from a reference genome [51–53]. Following the suggested guidelines [51], we eliminated OTUs with NSTI values higher than 2.

To visualize the functional dispersion of morphologically healthy and WS-stressed abalone, PCoA plots based on fourth root normalized metabolic KEGG pathway counts were carried out using STAMP v. 2.1.3 [54]. Significant differences among enriched pathways (effect size > 2) were evaluated by a Welch test implemented in STAMP v. 2.1.3 [54].

Results

Bioinformatics

Pyrosequencing returned 243,636 and 152,354 demultiplexed *16S rRNA* reads for HF and HC, respectively. Among them, 228,058 and 140,958 reads met quality criteria and were assigned to 790 and 596 OTUs for HF and HC, respectively. Rarefaction curves and Chao1 estimates suggest that we were able to sample the major fraction of the bacterial communities in both species given the asymptotic shape of the curves, the similarity between the asymptotic number of taxa for HF and HC, and the Chao1 estimates for both species (Additional File 2: Fig. S1c). All samples passed data quality control tests; however, 4 HF and 3 HC abalone individuals returned a lower number of reads than the selected rarefaction depth threshold

and were excluded from subsequent analyses. After read-rarefaction a total number of 590 and 448 bacteria-OTUs were obtained for HF and HF, respectively (Additional file 1: Table S3 and Table S4).

Microbiota structural composition

As we previously reported [33], *Tenericutes* was by far the predominant bacterial phylum in both morphologically healthy and WS-stressed abalone of both species. Moreover, both HF and HC possessed similar community structures at the highest taxonomic resolution. Most OTUs were assigned to four phyla (average abundance %): *Tenericutes* (HC: 60.2%, HF: 76.4%), *Proteobacteria* (HC: 24.1%, HF: 11.2%), *Fusobacteria* (HC: 3.8%, HF: 6.0%), and *Spirochaetes* (HC: 9.6%, HF: 3.9%).

Overall, WS-stressed organisms of both species were characterized by smaller contributions of *Mollicutes* to the total number of OTUs and read percentages. Nevertheless, both species differed in read-abundance patterns of non-*Mollicutes* taxa between healthy and WS-stressed specimens. Specifically, the majority of non-*Mollicutes* taxa increased congruently with regard to the number of OTUs and the percentage of total reads in WS-stressed HF abalone (Table 1). In contrast, the number of OTUs and read percentages from *Mollicutes* as well as most bacterial taxa decreased in WS-stressed HC abalone. Furthermore, these alpha-diversity changes were not followed by congruent changes in the number of reads. For example, *Alphaproteobacteria* showed a slight decrease in diversity (7% of OTUs) but contributed 2-fold the total number of reads in WS-stressed HC compared to that of *Spirochaetia*, *Fusobacteriia* and *Gammaproteobacteria* (Table 1). Notably, significant shifts in microbiome compositions were observed between healthy and WS-stressed HF abalone (PERMANOVA; pseudo-f: 3.1358; $p < 0.0322$), whereas no consistent structural changes were observed in healthy and diseased HC abalone.

Similar abundance patterns were also observed at the OTU taxonomic level. WS-stressed HF abalone possessed a higher fraction of exclusive bacterial OTU species than morphologically healthy animals (Fig. 1a and b), which resulted in increased microbial diversity (H' healthy= 2.4 and H' WS-stressed = 2.7). The LEfSe analysis revealed that 33 *Mollicutes* OTUs were either exclusive or predominant in either healthy or WS-stressed HF abalone (Additional file 1: Table S5). Moreover, the results of the SIMPER analysis revealed that total cumulative dissimilarity was mainly explained by the previous *Mollicutes* OTUs (55%) rather than by the presence of pathogenic bacteria, such as *C*Xc (Additional file 1: Table S5). The PCoA analysis based on Bray-Curtis and weighted Unifrac distance metrics revealed a significant structural differentiation of the bacterial communities between healthy and WS-stressed abalone (PERMANOVA; pseudo-f: > 4.88; $p < 0.0018$; Fig. 2a and Fig. 2b). In addition, WS-stressed HF presented a significant increase of multivariate dispersion (51.50 ± 1.5) compared to that of healthy organisms (43.50 ± 2.7; PERMDISP, F: 6.3706, $p = 0.0316$). On the contrary, a higher number of bacterial OTU species were detected among healthy HC abalone compared to that of WS-stressed HC despite no significant structural changes being observed among the microbiotas of HC abalone (Fig. 2c and 2d; Fig.3a and b). Moreover, differences in the presence or absence and/or OTU read abundance were observed in only 18 OTU species among healthy and WS-stressed HC, most of which were assigned to *Mycoplasma*

(Additional file 1: Table S6). Finally, similar multivariate dispersion patterns were observed between healthy (56.30 ± 1.3) and WS-stressed (56.33 ± 2.6) HC abalone.

Functional microbiome capabilities

Functional predictions where estimated for 524 and 529 bacterial OTU species for HF and HC, respectively. The remaining OTUs (n = 266 and n = 67 for HF and HC, respectively) were removed as they presented NSTI values > 2. Overall, a total of 152 and 141 functional pathways were predicted for HF and HC, respectively (Additional file 1: Table S7 and Table S8). According to KEGG hierarchical level 1, a similar abundance of functional pathways was observed among the tested abalone species and morphological conditions (Additional file 1: Table S7 and Table S8). Microbiota functional capability was mainly involved in metabolic pathways (up to 73%) with *Mycoplasma* being by far the main bacterial genus responsible for those functions in both healthy and WS-stressed abalone. Specifically, the bacterial genera presenting higher functional contributions (threshold > 1%) were *Mycoplasma* (92.9%), *Vibrio* (2.7%), and *Mesoplasma* (1.4%) in HF abalone and *Mycoplasma* (63.56%), *Spirochaeta* (11.87), *Mesoplasma* (4.51%), and *Vibrio* (3.54%) in HC.

The PCoA analyses performed using the normalized count numbers of the pathways (or KEGG level 3) revealed a significant functional split between healthy and WS-stressed HF abalone (Fig. 4a; PERMANOVA; pseudo-f: 6.77; p = 0.0018). This separation was explained by 79 of the 152 predicted pathways that presented significant differences in the mean proportion of WS-stressed and healthy HF abalone (Fig. 4b). Notably, under-expressed pathways (n = 59; Fig. 3b) in WS-stressed abalone were mainly related with metabolic activities, such as carbohydrate metabolism, amino acid metabolism, glycan biosynthesis, metabolism, and the metabolism of cofactors and vitamins (KEGG level 2; Fig. 3b). Most of the over-expressed genes (n = 20) in WS-stressed HF abalone were related with antibacterial and/or defense mechanisms like cellular apoptosis and antibacterial compound production (Fig. 3b). In contrast, no consistent differences were observed between the predicted pathways of WS-stressed and healthy HC abalone (PERMANOVA; pseudo-f: 2.40; p = 0.089). Moreover, the Welch test results revealed no significant differences in the normalized count number of the pathways between healthy and WS-stressed HC abalone.

Discussion

Overall, our findings suggest that WS may involve specific response patterns with regard to the structural and functional capabilities of the tested microbiotas. Notably, the extent to which WS may be associated with structural changes strongly depends on the configuration of the original unstressed microbiotas, as we observed significant alterations in less complex microbiotas (e.g., HF) while marginal changes were detected as bacterial diversity increased (e.g., HC). In this context, the results obtained between healthy and WS-stressed HF strongly support the AKP, as a higher number of both bacterial OTU species and

alternative configurations were observed in dysbiotic microbiotas [20]. Conversely, WS-stressed HC abalone generally presented a reduction in bacterial α-diversity.

These distinctive structural microbiota responses resulted in unequal shifts in functional capabilities. Specifically, no consistent functional alterations were observed in HC, whereas WS-stressed HF abalone showed a significant downregulation of several molecular pathways. The simplest explanation of this downregulation may be found in the Insurance hypotheses that have stated that higher diversity leads to more stable systems, which has been associated with species-specific responds to perturbation and functional redundancy [24–26]. Indeed, in a redundant system, the removal of species may not necessary result in a loss of functionality of the entire system, as other taxonomic groups may carry out the ecological tasks of the species that are removed [27]. This was particular evident in HC, where a higher number of bacterial OTU species were found to enrich the same KEGG pathway [33]; thus, reduced bacterial diversity does not necessarily result in a functional misregulation of the entire microbiota. On the other hand, from a functional prospective, the increase in α-diversity observed in WS-stressed HF should be considered to be stochastic, as predicted by the AKP. Indeed, the acquisition of additional bacterial taxa did not result in either an increase in functional capabilities or in the upregulation of predicted ecological pathways.

These results may be used to elucidate some aspects of WS that remain poorly understood. For instance, the different degrees of susceptibility to WS that have been observed among abalone species [15,34,55] may be related with the complexity level of each abalone species GI bacterial community. In this context, both a lower microbial diversity and a higher degree of susceptibility to WS (up to 100%) have been previously reported for HF; conversely, the higher bacterial α-diversity of HC may explain its lower susceptibility to WS (up to 60%) [33,34]. Recent advances have indicated that more complex microbiotas lead to more efficient systems and improved health conditions [27]. For example, a high microbiota diversity may reduce the susceptibility of individuals to infectious diseases through both direct and indirect mechanisms. Indeed, resident microbiotas may outcompete pathogens for space, metabolites, and nutrients [23,56] or inhibit and even kill pathogens via metabolic byproducts (e.g., bacteriocins, acids, and peptides) [57,58]. This may be particularly important in abalone, as higher interspecific microbiota diversity is generally explained by an increase in *Alpha-* and *Gammaproteobacteria* [6,33,59], both of which represent the main taxonomic groups that produce antimicrobial compounds in abalone species [60,61]. Thus, we posit that the lower susceptibility to WS observed in HC may be explained by both a high prevalence of *Alpha-* and *Gammaproteobacteria* [33] and the production of associated byproducts. Nevertheless, additional efforts are needed to validate this hypothesis.

Despite the aforementioned structural and functional differences, the taxonomic differences between the healthy and WS-stressed microbiotas from both abalone species were mainly attributed to changes in *Mycoplasma* abundance rather than the presence of pathogenic bacteria, such as *C*Xc. In this context, the GI microbiotas of all abalone were dominated by *Mycoplasma* and consequently the differences in the abundance of this bacterial group explained the largest dissimilarity among healthy and WS-stressed specimens. Moreover, although a significant increase of *C*Xc was observed in WS-stressed HF abalone, its

contribution to the total dissimilarity among morphological categories was generally low, ranging from 0.03–2.87%. In addition, *Proteobacteria* significantly increased in abundance in WS-affected abalone, suggesting that the increase in those bacteria may have resulted from opportunistic responses under unhealthy conditions. Together, these abundance patterns may indicate that the occurrence of WS may be primarily associated with a comprehensive change in the bacterial community or at least with a decrease in the number of certain *Mycoplasma* species [32], which in turn may result in functional shifts in dysbiotic microbiotas. This may be particularly true considering some ecological and biological characteristics of *Mycoplasma.* For example, the genomes of these microorganisms present a high number of genes involved in the degradation of glycans, proteins, and complex oligosaccharides [62,63]. Hence, as we previously proposed, the high number of detected *Mycoplasma* OTUs from both abalone species may indicate that this genus may be highly host-specific and that different *Mycoplasma* may bear some degree of specificity to particular metabolic functions and/or to specific steps along metabolic routes [32,33]. In addition, *Mycoplasma* may prevent infection from microbial pathogens in host species. Indeed, as *Mycoplasma* adhere and colonize epithelial GI tracts [64], they may physically prevent infection through the competitive inhibition for surface binding sites on cells [32]. In addition, the presence of some sialic acid lyase genes in the genomes of certain *Mycoplasma* species suggest that these bacteria may also prevent infection by breaking down the sialic acid residues of outer membrane proteins used by microbial pathogens to avoid the innate immune responses of hosts [62,65].

Finally, the assessment of microbiota structural and functional changes of this study may provide a new point of view to understand WS expression. Additional experimental evidence is required to complement and test the functional predictions of our in silico analyses. Moreover, the main challenge in predicting the ecological functions of the abalone microbiotas is related to their biological novelty. Indeed, up to 30% of detected bacterial OTUs were not included in our ecological prediction analysis because they presented low genetic similarity with database reference genomes (NASTI values > 2), implying their being new to science. Nevertheless, our main findings concern the differences between morphologically healthy and WS-stressed abalone and do not rely as much on the accuracy of microbiome prediction but rather on the precision required to differentiate among them. In this regard, our data have been shown to be consistent. In addition, no structural or functional changes were observed between HC abalone with and without morphological signs of WS. The simplest explanation may be that a low number of HC abalone were harvested that presented morphological signs of WS. However, as suggested by the same authors that proposed the AKP, several biological patterns may conceal this principle [20]. Hence, additional explanations may be considered. Our results support the presence of seasonally distinct microbiotas in HC. Seasonal variation in microbiotas have been previously reported in other abalone species [6,28]. It is likely that those seasonal changes may have been driven by diet [28], and we posit that they may confer an adaptive value to abalone. Indeed, it is reasonable to assume that abalone diets vary according to seasonal food availability, among other factors, and that this may drive changes in GI microbiotas that are beneficial to hosts. Nevertheless, the analysis of seasonal microbiota changes is outside the scope of this study and was not directly addressed. However, the integration of this

information may help to further the understanding of the occurrence of WS and should be considered in further investigations.

Conclusions

Gastro-intestinal microbiota diversity appears to play a pivotal role in both (*i*) the health of abalone spp. and (*ii*) the etiology of WS. Notably, significant structural and functional alterations were detected in less complex microbiotas. In those microbiotas, structural changes appeared to be stochastic, as they were followed by the down-regulation of essential metabolic pathways conducted by GI bacteria. Conversely, more complex microbiotas appeared marginally affected by WS in terms of both structural and functional capabilities. The latter may be explained by the prediction that highly complex communities are highly stable, as different species may deferentially respond to perturbations and/or carry out the same ecological function (e.g., functional redundancy). In agreement with these observations, we propose that the species-specific degree of susceptibility to WS may be related with the degree of complexity of the GI bacterial communities harbored by each abalone species; nevertheless, additional studies are needed to test this hypothesis.

Abbreviations

bacterial tag-encoded FLX amplicon pyrosequencing (bTEFAP), *Candidatus* Xenohaliotis californiensis (CXc), gastro-intestinal (GI), *Haliotis fulgens* (HF), *Haliotis corrugata* (HC), healthy (no-WS), Kyoto Encyclopedia of Genes and Genomes (KEGG), linear discriminant analysis (LDA) effect size (LEfSe), multiplex identifier (MID), National Center for Biotechnology Information (NCBI), nearest sequenced taxon index (NSTI), operational taxonomic unit (OTU), permutation analysis of multivariate dispersion (PERMDISP), permutational multivariate analysis of variance (PERMANOVA), principal coordinate analysis (PCoA), Quantitative Insights Into Microbial Ecology (QIIME), similarity percentage (SIMPER), withering syndrome (WS), WS-stressed (WS-stressed)

Declarations

Ethics approval and consent to participate

Not applicable

Consent for publication

Not applicable

Competing interests

The authors declare that they have no competing interests

Funding

This study as supported by SAGARPA-CONACYT [grant number 2011-C01-163322], UC Mexus-CONACYT [grant number CN-14-14], and the Fund for Scientific Research and Technological Development of CICESE [grant number FID-2012-01]. The first author received a graduate fellowship from CONACYT to support his Ph.D. research in Marine Ecology at the Centro de Investigación Científica y de Educación Superior de Ensenada (CICESE).

Author Contributions

Conceptualization: FC, JDM and ARO; Data curation: FC, JACC, MP and JS; Formal analysis: FC, JACC, MP and JS; Funding acquisition: ARO and JDM; Investigation: FC and ARO; Methodology: FC, JACC, MP, JS; Project administration: ARO; Resources: ARO and JDM; Software: FC, JACC, MP and JS; Supervision: FC, ARO and JDM; Validation: FC, JACC, MP, JS, JDM and ARO; Visualization: FC; Writing – original draft: FC; Writing – review & editing: FC, JACC, MP, JS, JDM and ARO.

Acknowledgements

We are grateful to Dr. W. Kelley Thomas for providing us with the possibility of running bio-informatics pipelines using the server of the Research Computing Center of the University of New Hampshire and Andrea Lievana-MacTavish for a critical assessment of an earlier version of the manuscript and English editing.

Availability of data and materials

Raw reads were deposited in the National Center for Biotechnology Information (NCBI; BioProject: PRJNA494699, accession number: SRR7969002).

References

1. Moore JD, Byron SN, Marshman BC, Snider JP. An oxytetracycline bath protocol to eliminate the agent of withering syndrome, *Candidatus* Xenohaliotis californiensis, in captive abalone populations. Aquaculture. Elsevier; 2019;503:267–74.
2. Miner CM, Altstatt JM, Raimondi PT, Minchinton TE. Recruitment failure and shifts in community structure following mass mortality limit recovery prospects of black abalone. Mar Ecol Prog Ser. 2006;327:107–17.

3. Crosson LM, Friedman CS. Withering syndrome susceptibility of northeastern Pacific abalones: A complex relationship with phylogeny and thermal experience. J Invertebr Pathol. Elsevier; 2018;151:91–101.
4. Cox KW. California Abalones, Family Haliotidae. Fish Bull No 118. 1962;118:1–131.
5. Mateos HT, Lewandowski PA, Su XQ. Seasonal variations of total lipid and fatty acid contents in muscle, gonad and digestive glands of farmed Jade Tiger hybrid abalone in Australia. Food Chem. Elsevier Ltd; 2010;123:436–41.
6. Lee MJ, Lee JJ, Han YC, Sang HC, Kim BS. Analysis of microbiota on abalone (*Haliotis discus hannai*) in South Korea for improved product management. Int J Food Microbiol. Elsevier; 2016;234:45–52.
7. Vater A, Byrne BA, Marshman BC, Ashlock LW, Moore JD. Differing responses of red abalone (*Haliotis rufescens*) and white abalone (*H. sorenseni*) to infection with phage-associated *Candidatus* Xenohaliotis californiensis. PeerJ. 2018;6:e5104.
8. Morales-Bojórquez E, Muciño-Díaz MO, Vélez-Barajas JA. Analysis of the Decline of the Abalone Fishery (*Haliotis fulgens* and *H. corrugata*) along the Westcentral Coast of the Baja California Peninsula, Mexico. J Shellfish Res. 2008;27:865–70.
9. SAGARPA. Sustentabilidad y Pesca Responsable en México. Evaluación y Manejo. 2009.
10. Valles-Ríos H. Análisis histopatológico del abulón negro *Haliotis cracherodii* afectado por el síndrome de deterioro. Cienc Pesq. 2000;14:5–19.
11. Cáceres-Martínez J, Vásquez-Yeomans R, Flores-Saaib RD. Intracellular prokaryote Xenohaliotis californiensis in abalone *Haliotis* spp. from Baja California, México. Cienc Pesq. 2011;19:5–11.
12. Cicala F, Moore JD, Cáceres-Martínez J, del Río-Portilla MA, Hernández-Rodríguez M, Vásquez Yeomans R, et al. Multigenetic characterization of '*Candidatus* Xenohaliotis californiensis.' Int J Syst Evol Microbiol. 2017;67:42–9.
13. Friedman CS, Andree KB, Beauchamp KA, Moore JD, Robbins TT, Shields JD, et al. '*Candidatus* Xenohaliotis californiensis', a newly described pathogen of abalone, *Haliotis* spp., along the west coast of North America. Int J Syst Evol Microbiol. 2000;50:847–55.
14. Cáceres-Martínez J, Tinoco-Orta GD. Symbionts of cultured red abalone *Haliotis rufescens* from Baja California, Mexico [Internet]. J. Shellfish Res. 2001. p. 875–81.
15. Álvarez Tinajero MDC, Cáceres-Martínez J, Gonzáles Avilés JG, Del Carmen Alvarez Tinajero M, Caceres-Martinez J, Aviles JGG. Histopathological evaluation of the yellow abalone *Haliotis corrugata* and the blue abalone *Haliotis fulgens* from Baja California, México. J. Shellfish Res. 2002. p. 825–30.
16. Balseiro P, Aranguren R, Gestal C, Novoa B, Figueras A. *Candidatus* Xenohaliotis californiensis and *Haplosporidium montforti* associated with mortalities of abalone *Haliotis* tuberculata cultured in Europe. Aquaculture. 2006;258:63–72.
17. Horwitz R, Mouton A, Coyne VE. Characterization of an intracellular bacterium infecting the digestive gland of the South African abalone *Haliotis midae*. Aquaculture. Elsevier; 2016;451:24–32.

18. Nicolas JL, Basuyaux O, Mazurié J, Thébault A. *Vibrio carchariae*, a pathogen of the abalone *Haliotis tuberculata*. Dis Aquat Organ. 2002;50:35–43.
19. McFall-Ngai M, Hadfield MG, Bosch TCG, Carey H V., Domazet-Lošo T, Douglas AE, et al. Animals in a bacterial world, a new imperative for the life sciences. Proc Natl Acad Sci U S A. 2013;110:3229–36.
20. Zaneveld JR, McMinds R, Thurber RV. Stress and stability: Applying the Anna Karenina principle to animal microbiomes. Nat Microbiol. 2017;2:1–8.
21. Sharon G, Segal D, Ringo JM, Hefetz A, Zilber-Rosenberg I, Rosenberg E. Commensal bacteria play a role in mating preference of *Drosophila melanogaster*. Proc Natl Acad Sci U S A. 2010;107:20051–6.
22. Hsiao EY, McBride SW, Hsien S, Sharon G, Hyde ER, McCue T, et al. Microbiota modulate behavioral and physiological abnormalities associated with neurodevelopmental disorders. Cell. Elsevier Inc.; 2013;155:1451–63.
23. Libertucci J, Young VB. The role of the microbiota in infectious diseases. Nat Microbiol. Springer US; 2019;4:35–45.
24. Yachi S, Loreau M. Biodiversity and ecosystem productivity in a fluctuating environment: The insurance hypothesis. Proc Natl Acad Sci U S A. 1999;96:1463–8.
25. Konopka A. What is microbial community ecology. ISME J. 2009;3:1223–30.
26. Mccann KS. The diversity–stability debate. Nature. 2000;405:228–33.
27. Larsen OFA, Claassen E. The mechanistic link between health and gut microbiota diversity. Sci Rep. Springer US; 2018;8:6–10.
28. Gobet A, Mest L, Perennou M, Dittami SM, Caralp C, Coulombet C, et al. Seasonal and algal diet-driven patterns of the digestive microbiota of the European abalone *Haliotis tuberculata*, a generalist marine herbivore. Microbiome. Microbiome; 2018;6:60.
29. Le Roux F, Wegner KM, Polz MF. Oysters and Vibrios as a Model for Disease Dynamics in Wild Animals. Trends Microbiol. Elsevier Ltd; 2016;24:568–80.
30. Zaneveld JR, Burkepile DE, Shantz AA, Pritchard CE, McMinds R, Payet JP, et al. Overfishing and nutrient pollution interact with temperature to disrupt coral reefs down to microbial scales. Nat Commun. 2016;7:1–12.
31. Lesser MP, Fiore C, Slattery M, Zaneveld J. Climate change stressors destabilize the microbiome of the Caribbean barrel sponge, *Xestospongia muta*. J Exp Mar Bio Ecol. Elsevier B.V.; 2016;475:11–8.
32. Villasante A, Catalán N, Rojas R, Lohrmann KB, Romero J. Microbiota of the digestive gland of red abalone (*Haliotis rufescens*) is affected by withering syndrome. Microorganisms. 2020;8:1–13.
33. Cicala F, Cisterna-Celiz JA, Moore JD, Rocha-Olivares A. Structure, dynamics and predicted functional ecology of the gut microbiota of the blue (*Haliotis fulgens*) and yellow (*H . corrugata*) abalone from Baja California Sur, Mexico. PeerJ. 2018;5:e3233v1.
34. Friedman CS. Infection with Xenohaliotis californiensis. Man Diagnostic Tests Aquat Anim. 2012;511–23.

35. Ludwig W, Mittenhuber G, Friedrich CG. Transfer of *Thiosphaera pantotropha* to *Paracoccus denitrificans*. Int J Syst Bacteriol. 1993;43:363–7.
36. Ruff-Roberts AL, Kuenen JG, Ward DM. Distribution of cultivated and uncultivated cyanobacteria and *Chloroflexus*-like bacteria in hot spring microbial mats. Appl Environ Microbiol. 1994;60:697–704.
37. Dowd SE, Callaway TR, Wolcott RD, Sun Y, McKeehan T, Hagevoort RG, et al. Evaluation of the bacterial diversity in the feces of cattle using 16S rDNA bacterial tag-encoded FLX amplicon pyrosequencing (bTEFAP). BMC Microbiol. 2008;8:125.
38. Edgar RC. Search and clustering orders of magnitude faster than BLAST. Bioinformatics. 2010;26:2460–1.
39. Bolyen E, Rideout J, Dillon M, Bokulich N, Abnet C, Al-Ghalith G, et al. Reproducible, interactive, scalable and extensible microbiome data science using QIIME 2. Nat Biotechnol. 2019;37:852–7.
40. Rognes T, Flouri T, Nichols B, Quince C, Mahé F. VSEARCH: a versatile open source tool for metagenomics. PeerJ. 2016;4:e2584.
41. Edgar RC, Haas BJ, Clemente JC, Quince C, Knight R. UCHIME improves sensitivity and speed of chimera detection. Bioinformatics. 2011;27:2194–200.
42. Camacho C, Coulouris G, Avagyan V, Ma N, Papadopoulos J, Bealer K, et al. BLAST+: Architecture and applications. BMC Bioinformatics. 2009;10:1–9.
43. Quast C, Pruesse E, Yilmaz P, Gerken J, Schweer T, Yarza P, et al. The SILVA ribosomal RNA gene database project: Improved data processing and web-based tools. Nucleic Acids Res. 2013;41:590–6.
44. Bokulich NA, Subramanian S, Faith JJ, Gevers D, Gordon I, Knight R, et al. Quality-filtering vastly improves diversity estimates from Illumina amplicon sequencing. Nat Methods. 2013;10:57–9.
45. Chao A. Nonparametric Estimation of the Number of Classes in a Population. Scanadinavian J Stat. 1984;11:265–70.
46. Vázquez-Baeza Y, Pirrung M, Gonzalez A, Knight R. EMPeror : a tool for visualizing high-throughput microbial community data. Gigascience. 2013;2:1–4.
47. Anderson MJ. A new method for non-parametric multivariate analysis of variance. Austral Ecol. 2001;26:32–46.
48. Clarke KR, Warwick RM. A further biodiversity index applicable to species lists: Variation in taxonomic distinctness. Mar Ecol Prog Ser. 2001;216:265–78.
49. Heberle H, Meirelles VG, da Silva FR, Telles GP, Minghim R. InteractiVenn: A web-based tool for the analysis of sets through Venn diagrams. BMC Bioinformatics. 2015;16:1–7.
50. Segata N, Izard J, Waldron L, Gevers D, Miropolsky L, Garrett WSW, et al. Metagenomic biomarker discovery and explanation. Genome Biol. 2011;12:1–18.
51. Douglas GM, Maffei VJ, Zaneveld J, Yurgel SN, Brown JR, Taylor CM, et al. PICRUSt2: An improved and extensible approach for metagenome inference. BioRxiv. 2019;1–42.

52. Langille M, Zaneveld J, Caporaso JG, McDonald D, Knights D, Reyes J, et al. Predictive functional profiling of microbial communities using 16S rRNA marker gene sequences. Nat Biotechnol. Nature Publishing Group; 2013;31:814–21.
53. de Voogd NJ, Cleary DFR, Polónia ARM, Gomes NCM. Bacterial community composition and predicted functional ecology of sponges, sediment and seawater from the thousand islands reef complex, West Java, Indonesia. FEMS Microbiol Ecol. 2015;91:1–12.
54. Parks DH, Tyson GW, Hugenholtz P, Beiko RG. STAMP: Statistical analysis of taxonomic and functional profiles. Bioinformatics. 2014;30:3123–4.
55. Moore JD, Juhasz CI, Robbins TT, Ignacio Vilchis L. Green abalone, *Haliotis fulgens* infected with the agent of withering syndrome do not express disease signs under a temperature regime permissive for red abalone, *Haliotis rufescens*. Mar Biol. 2009;156:2325–30.
56. Abt MC, Pamer EG. Commensal bacteria mediated defenses against pathogens. Curr Opin Immunol. 2014;29:16–22.
57. Rea MC, Sit CS, Clayton E, O'Connor PM, Whittal RM, Zheng J, et al. Thuricin CD, a posttranslationally modified bacteriocin with a narrow spectrum of activity against *Clostridium difficile*. Proc Natl Acad Sci U S A. 2010;107:9352–7.
58. Harris VC, Haak BW, Boele van Hensbroek M, Wiersinga WJ. The Intestinal Microbiome in Infectious Diseases: The Clinical Relevance of a Rapidly Emerging Field. Open Forum Infect Dis. 2017;4:1–8.
59. Iehata S, Nakano M, Tanaka R, Maeda H. Modulation of gut microbiota associated with abalone *Haliotis gigantea* by dietary administration of host-derived *Pediococcus* sp. Ab1. Fish Sci. 2014;80:323–31.
60. Offret C, Jégou C, Mounier J, Fleury Y, Le Chevalier P. New insights into the haemo- and coelo-microbiota with antimicrobial activities from Echinodermata and Mollusca. J Appl Microbiol. 2019;126:1023–31.
61. Offret C, Rochard V, Laguerre H, Mounier J, Huchette S, Brillet B, et al. Protective Efficacy of a Pseudoalteromonas Strain in European Abalone, *Haliotis tuberculata*, Infected with *Vibrio harveyi* ORM4. Probiotics Antimicrob Proteins. Probiotics and Antimicrobial Proteins; 2019;11:239–47.
62. Wang Y, Huang JM, Wang SL, Gao ZM, Zhang AQ, Danchin A, et al. Genomic characterization of symbiotic mycoplasmas from the stomach of deep-sea isopod bathynomus sp. Environ. Microbiol. 2016.
63. Birhanu AG, Yimer SA, Kalayou S, Riaz T, Zegeye ED, Holm-Hansen C, et al. Ample glycosylation in membrane and cell envelope proteins may explain the phenotypic diversity and virulence in the Mycobacterium tuberculosis complex. Sci Rep. 2019;9:1–15.
64. Henrich B, Feldmann RC, Hadding U. Cytoadhesins of Mycoplasma hominis. Infect Immun. 1993;61:2945–51.
65. Severi E, Hood DW, Thomas GH. Sialic acid utilization by bacterial pathogens. Microbiology. 2007;153:2817–22.

Table

Table 1 is available in the Supplementary Files

Figures

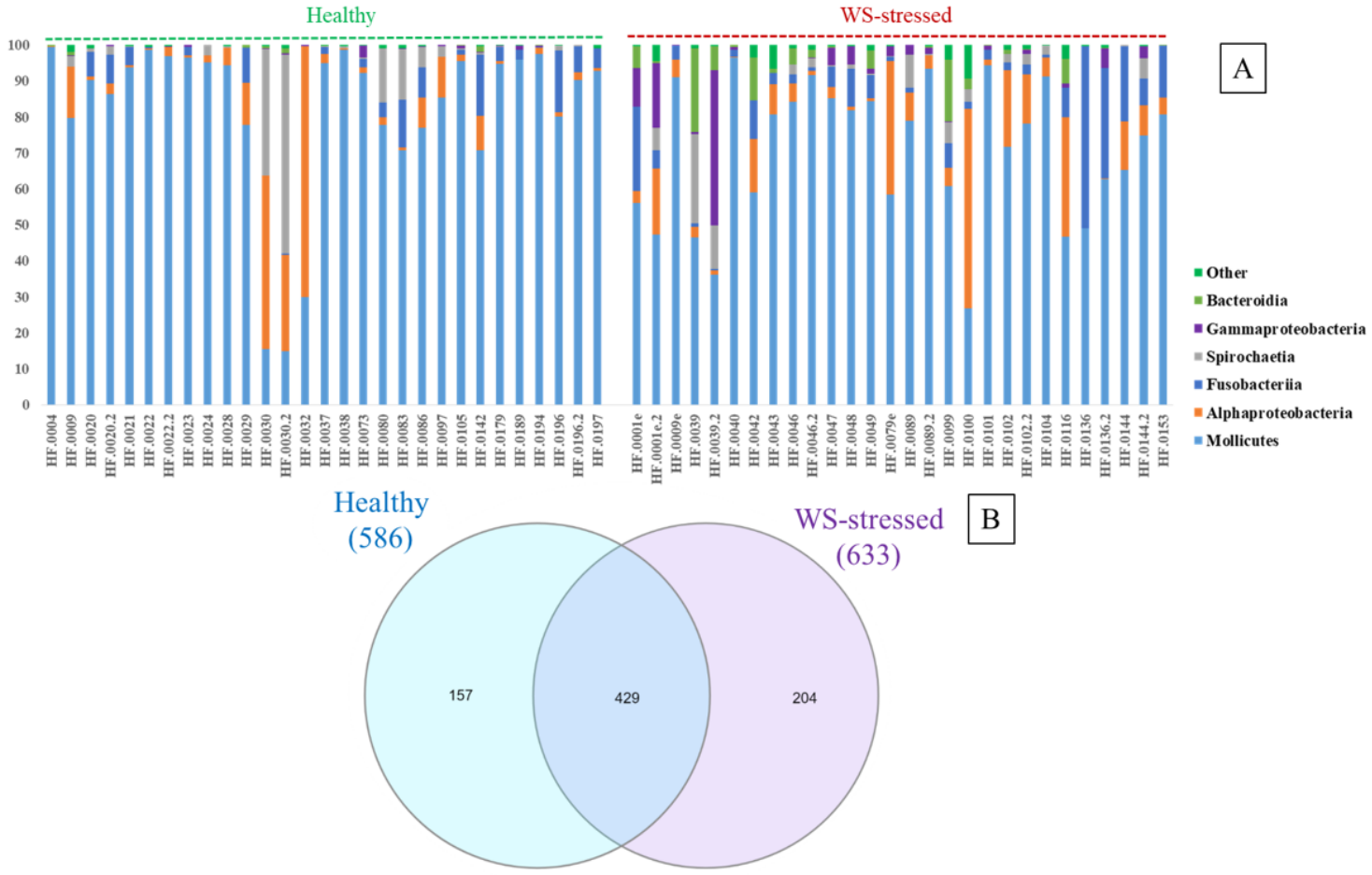

Figure 1

Haliotis fulgens gastro-intestinal tract microbiota composition. Major bacterial taxa comprising the gut microbiota [A] and Venn diagram of the number of exclusive and/or common operational taxonomic units (OTUs) [B] in healthy and WS-stressed H. fulgens (HF).

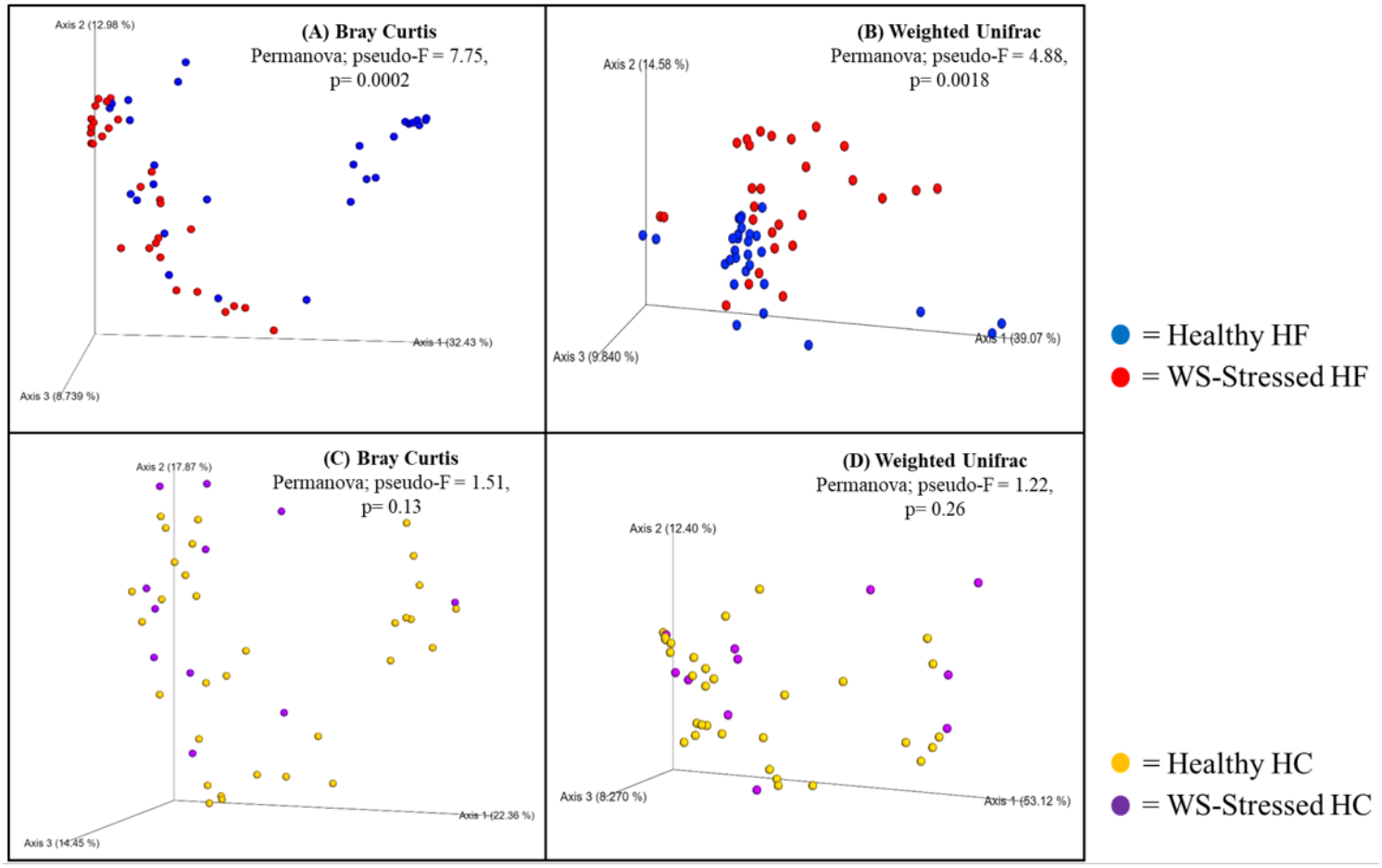

Figure 2

Microbiome structural variation. Principal coordinate analysis (PCoA) based on four distance metrics. The PCoAs were obtained using assigned operational taxonomic units (OTUs) assembled at a 97% similarity cut-off for the gut microbiota of Haliotis fulgens (HF) and Haliotis corrugata (HC).

Figure 3

Haliotis corrugata gastro-intestinal tract microbiota composition. Major bacterial taxa comprising the gut microbiota [A] and Venn diagram of the number of exclusive and/or operational taxonomic units (OTUs) [B] in healthy and WS-stressed H. corrugata (HC).

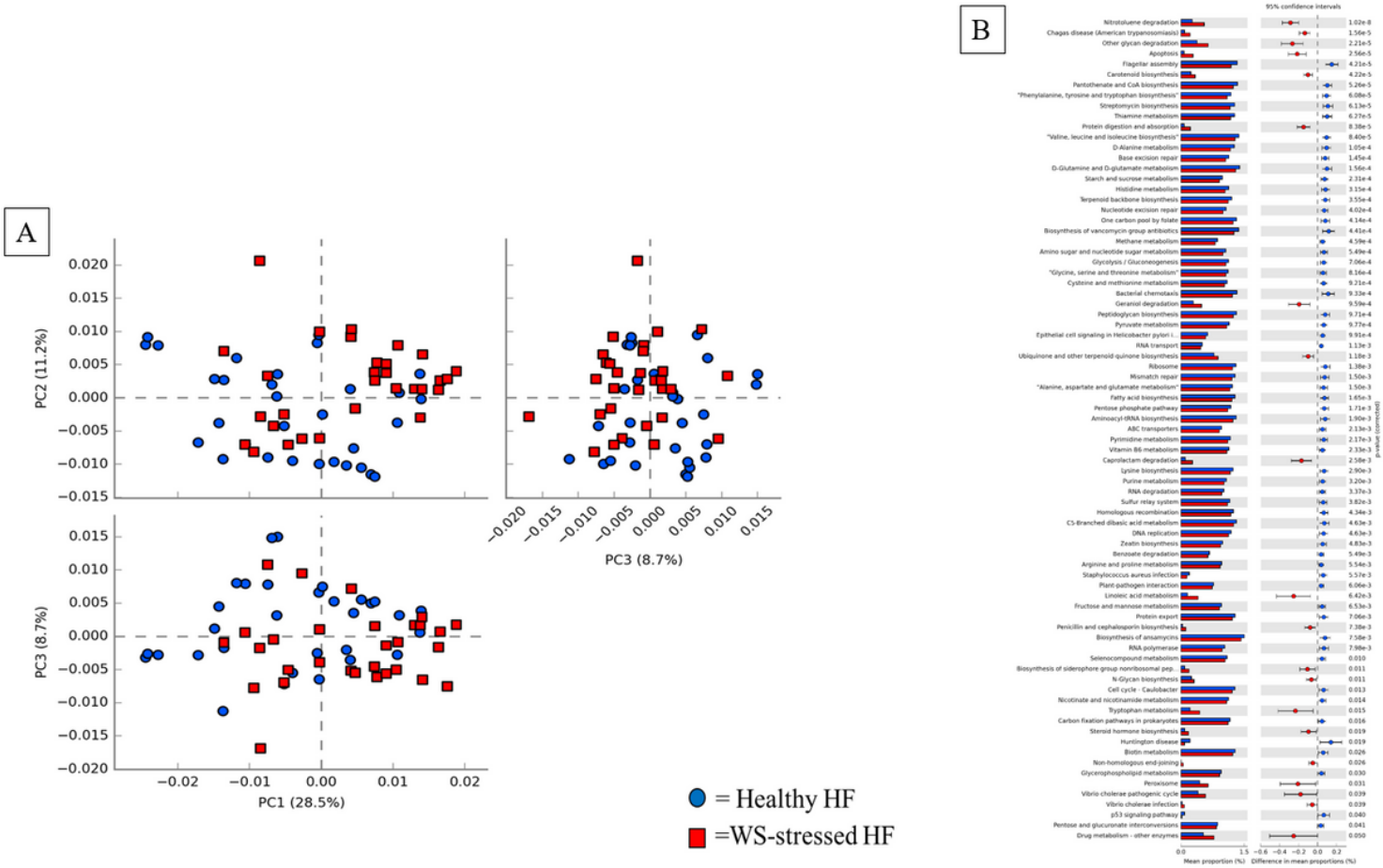

Figure 4

Microbiome functional variation in Haliotis fulgens (HF). Principal coordinate analysis (PCoA) based on the Kyoto Encyclopedia of Genes and Genomes (KEGG) pathway abundances [A]. Difference in the functional mean proportion between healthy and WS-stressed abalone [B].

Supplementary Files

This is a list of supplementary files associated with this preprint. Click to download.

- Table23.02.21.docx
- Additionalfile1S.Tables23.02.21.xlsx
- Additionalfile2S.Fig23.02.21.pptx